Photosensitive Self-Assembled Monolayers on Gold: Photochemistry of Surface-Confined Aryl Azide and Cyclopentadienylmanganese Tricarbonyl

Eric W. Wollman, Doris Kang, C. Daniel Frisbie, Ivan M. Lorkovic, and Mark S. Wrighton*

Contribution from the Department of Chemistry, Massachusetts Institute of Technology, Cambridge, Massachusetts 02139

Received July 19, 1993®

Abstract: Photosensitive self-assembled monolayers (SAMs) are prepared by the spontaneous reaction of di-11-(4-azidobenzoate)-1-undecyl disulfide, **I**, or 11-mercaptoundecylcyclopentadienylmanganese tricarbonyl, **II**, with polycrystalline Au. SAMs of **I** are photosensitive by virtue of a pendant aryl azide moiety (λ_{max} = 270 nm, log ϵ = 4.2) which undergoes photoreaction with secondary amines to form Au-confined derivatives of 3-H azepine and hydrazine, while Au-**II** SAMs undergo photosubstitution of phosphine for CO. Au-**I** SAMs irradiated in the presence of various secondary amines were characterized by reflection absorption infrared spectroscopy (RAIRS), XPS, and cyclic voltammetry, and showed persistent attachment of approximately one monolayer of amine. Infrared spectroscopy was used to establish that primary photoproducts obtained upon irradiation of Au-**I** SAMs in diethylamine are nearly identical to primary photoproducts obtained upon irradiating an analog of **I**, methyl 4-azidobenzoate, in diethylamine solution. XPS analysis of Au-**I** SAMs before and after irradiation in the presence of secondary amines confirms loss of N_2 from the Au-**I** SAM and incorporation of one nitrogen atom per surface-confined molecule. Most definitively, cyclic voltammetry of Au-**I** after irradiation in the presence of 2-ferrocenylethyl-2′,2′,2′-trifluoroethylamine, **III**, showed 3.3×10^{-10} mol cm^{-2} of surface-confined ferrocene. Positive ion SIMS spectra of Au-**II** irradiated in the presence of PPh_2Et, $PPh_2(n\text{-}Pr)$, $PPh_2(CH_2)_{11}Fc$, **X**, Fc = ferrocenyl, or $PPh_2(CH_2)_2(CF_2)_5CF_3$, **XI**, show that introduction of the phosphine onto the surface occurs upon near-UV irradiation. Importantly, the surface photochemistry of **I** and **II** allows the high lateral resolution patterning of Au surfaces and Au microstructures with a variety of molecular reagents. SIMS maps for vinyl ferrocenium (m/z 212) or F^- (m/z 19) of flat Au-**II** substrates irradiated through a Cr-on-glass mask in the presence of **X** or **XI** demonstrate photochemical patterning at a lateral resolution of <2 μm. SEM confirms the resolution of 2 μm features in the irradiated monolayer. Cyclic voltammetry and SIMS were used to demonstrate that Au microstructures derivatized with **I** can be patterned with molecular reagents, also at a lateral resolution of <2 μm by UV irradiation through a mask and a thin film of the desired amine. A condensation figure was used to demonstrate photopatterning of a flat Au-**I** substrate irradiated through a mask and a thin film of $(C_2H_5OH)_2NH$.

We report the formation, characterization, and photochemistry of self-assembled monolayers (SAMs)[1] of di-11-(4-azidobenzoate)-1-undecyl disulfide, **I**, on Au, Scheme 1. We also demonstrate that Au-**I** SAMS as well as those of 11-mercaptoundecylcyclopentadienylmanganese tricarbonyl (Au-**II**) may be used to photopattern Au surfaces and microstructures at better than 2 μm lateral resolution. Our goal is to exploit known solution photochemistry of the aryl azide and $(\eta^5\text{-}C_5H_5)Mn(CO)_3$ moieties to effect selective attachment of functionalized amines, such as **III**, Scheme 1, or phosphines to irradiated portions of a Au-**I** or Au-**II** SAM, respectively. Such chemistry provides a route to high lateral resolution patterning of surfaces with molecular reagents. Recently, there have been a number of reports on photochemical and mechanical methods for patterning monolayer films.[2-9] The motivation for these efforts lies in the enormous utility of patterned thin films for control of surface reactivity, as evidenced by use of thin films in patterned deposition or etching of bulk materials,[3] synthesis of surface-confined biopolymer arrays,[4] and directed cellular adhesion and growth.[3a,5] There are obvious connections between efforts to pattern monolayers and ongoing development of organic resists in microfabrication

* Author to whom correspondence should be addressed.

® Abstract published in *Advance ACS Abstracts*, March 1, 1994.

(1) (a) Nuzzo, R. G.; Allara, D. L. *J. Am. Chem. Soc.* **1983**, *105*, 4481. (b) Nuzzo, R. G.; Zegarski, B. R.; Dubois, L. H. *J. Am. Chem. Soc.* **1987**, *109*, 733. (c) Swalen, J. D.; Allara, D. L.; Andrade, J. D.; Chandross, E. A.; Garoff, S.; Israelachvili, J.; McCarthy, T. J.; Murray, R.; Pease, R. F.; Rabolt, J. F.; Wynne, K. J.; Yu, H. *Langmuir* **1987**, *3*, 932, and references therein. (d) Strong, L.; Whitesides, G. M. *Langmuir* **1988**, *4*, 546. (e) Wasserman, S. R.; Tao, Y.-T.; Whitesides, G. M. *Langmuir* **1989**, *5*, 1074. (f) Bain, C. D.; Whitesides, G. M. *J. Am. Chem. Soc.* **1989**, *111*, 7164. (g) Whitesides, G. M.; Laibinis, P. E. *Langmuir* **1990**, *6*, 87. (h) Chidsey, C. E. D.; Bertozzi, C. R.; Putvinski, T. M.; Mujsce, A. M. *J. Am. Chem. Soc.* **1990**, *112*, 4301. (i) Hickman, J. J.; Ofer, D.; Zou, C.; Wrighton, M. S.; Laibinis, P. E.; Whitesides, G. M. *J. Am. Chem. Soc.* **1991**, *113*, 1128. (j) Ulman, A. *An Introduction to Ultrathin Organic Films From Langmuir-Blodgett to Self-Assembly*; Academic Press: Boston, MA, 1991.

(2) (a) Abbott, N. L.; Folkers, J. P.; Whitesides, G. M. *Science* **1992**, 257, 1380. (b) Lopez, G. P.; Biebuyck, H. A.; Frisbie, C. D.; Whitesides, G. M. *Science* **1993**, 647.

(3) (a) Dulcey, C. S.; Georger, J. H., Jr.; Krauthamer, V.; Stenger, D. A.; Fare, T. L.; Calvert, J. M. *Science* **1991**, *252*, 551. (b) Calvert, J. M; Georger, J. H., Jr.; Peckerar, M. C.; Perhsson, P. E.; Schnur J. M.; Schoen, P. E. *Thin Solid Films* **1992**, *210/211*, 359. (c) Kumar, A.; Biebuyck, H. A.; Abbott, N. L.; Whitesides, G. M. *J. Am. Chem. Soc.* **1992**, *114*, 9188. (d) Dressick, W. J.; Dulcey, C. S.; Georger, J. H., Jr.; Calvert, J. M. *Chem. Mat.* **1993**, *5*, 148.

(4) (a) Fodor, S. P. A.; Read, J. L.; Pirrung, M. C.; Stryer, L.; Lu, A. T.; Solas, D. *Science* **1991**, *251*, 767. (b) Rozsnyai, L. F.; Benson, D. R.; Fodor, S. P. A.; Schultz, P. G. *Angew. Chem., Int. Ed. Engl.* **1992**, *31*, 759. (c) Bhatia, S. K.; Hickman, J. J.; Ligler, F. S. *J. Am. Chem. Soc.* **1992**, *114*, 4433.

(5) (a) Stenger, D. A.; Georger, J. H.; Dulcey, C. S.; Hickman, J. J.; Rudolf, A. S.; Nielsen, T. B.; McCort, S. M.; Calvert, J. M. *J. Am Chem. Soc.* **1992**, *114*, 8435. (b) Lòpez, G. P.; Albers, M. W.; Schreiber, S. L.; Carroll, R.; Peralta, E.; Whitesides, G. M. *J. Am. Chem. Soc.* **1993**, *115*, 5877.

(6) Calabrese, G. S.; Abali, L. N.; Bohland, J. F.; Pavelchek, E. K.; Sricharoenchaikit, P.; Vizvary, G.; Bobbio, S. M.; Smith, P. *Adv. in Resist Technol. Process. 8* **1991**, *1466*, 528.

(7) (a) Kang, D.; Wrighton, M. S. *Langmuir* **1991**, *7*, 2169. (b) Kang, D.; Wollman, E. W.; Wrighton, M. S. In *Photosensitive Metal-Organic Systems*; Kutal, C., Serpone, N., Eds.; Advances in Chemistry Series 238; American Chemical Society: Washington, DC, 1993; p 45.

(8) (a) Ross, C. B.; Sun, L.; Crooks, R. M. *Langmuir* **1993**, *9*, 632. (b) Kim, Y.-T.; Bard, A. J. *Langmuir* **1992**, *8*, 1096.

(9) Tarlov, M. J.; Burgess, D. R. F.; Gillen, G. *J. Am. Chem. Soc.* **1993**, *115*, 5305.

0002-7863/94/1516-4395$04.50/0

Scheme 1. Photochemistry of Au-I and Au-II SAMs Involving Surface Photoattachment of Functionalized Amines such as III and Phosphines, L

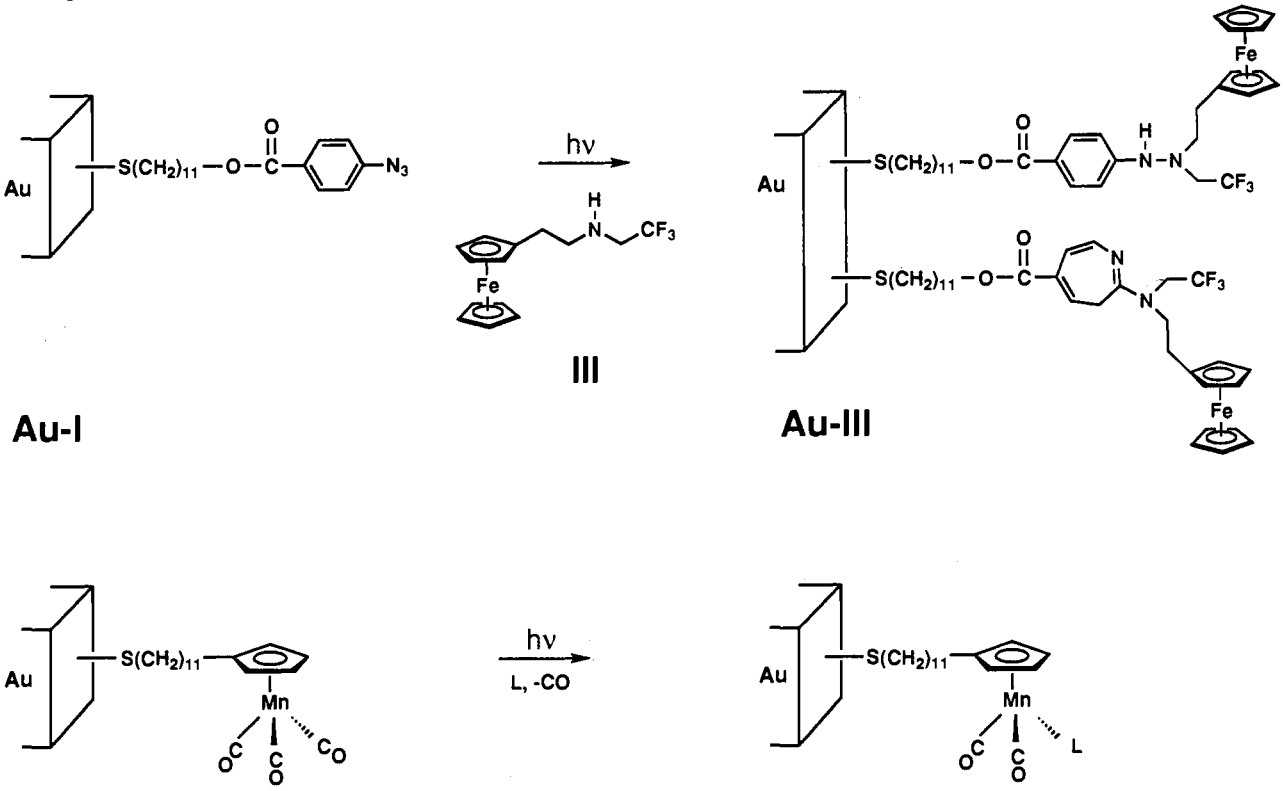

technology,[6] and indeed it has been shown that mechanically patterned SAMs can be used as monolayer resists for selective etching of some materials, such as Au.[3c]

Our work on photochemical methods for patterning SAMs has also been motivated by our prior experience in photolithography for microfabrication purposes. We have previously reported that Au-II SAMs can undergo photosubstitution of functionalized phosphines L for CO to give the corresponding Au-confined dicarbonylphosphines, Scheme 1.[7] The photochemistry of (η^5-C_5H_4R)$Mn(CO)_3$-containing SAMs is unique in that a single, well-characterized photoproduct is produced. In contrast, much of the work reported in the literature to date on photochemical patterning of SAMs has involved photoinduced decomposition of the SAM to yield uncharacterized surface-confined photoproducts. One exception is the recent work of Hemminger,[10ac] who has shown that under UV irradiation thiolates on Au will react with atmospheric H_2O or O_2 to produce sulfonate species in good yield. Tarlov has subsequently shown that this chemistry can be used to pattern SAMs of alkanethiols with ~20 μm resolution.[9] A goal in our laboratory has been to create photosensitive SAMs which undergo well-defined photoinduced reactions with functionalized molecules. Photopatterning a SAM in the presence of a well-defined trapping reagent opens the possibility of tailoring surfaces with a broad range of molecular functionality.

The solution photochemistry of aryl azides has been extensively studied[11-18] and is characterized by efficient ($\Phi > 0.5$, λ_{max} = 270 nm, log ϵ = 4.2) liberation of molecular nitrogen to form aryl nitrenes. In the presence of primary or secondary amines good yields of 3*H*-azepine and/or hydrazine amine trapped products are obtained, making aryl azide derivatives good candidates for efficient photomodification of surfaces. Photopatterning of bare insulator, semiconductor, and conducting polymer surfaces using aryl azide derivatives has been reported,[19] and workers in this laboratory have studied photopatterning of aryl azide-containing alkyltriethoxysilane SAMs on Si and metal oxide surfaces,[20] but the products formed in these studies were not clearly defined.

We demonstrate here that known solution photochemistry of aryl azides in the presence of amines can be extended to aryl azide-containing thiolate SAMs on Au, affording surface-confined primary photoproducts which are analogous to those obtained in solution. Together, aryl azide and (η^5-C_5H_4R)$Mn(CO)_3$ surface photochemistry represent a rational approach to the function-

(10) (a) Li, Y; Huang, J.; McIver, R. T.; Hemminger, J. C. *J. Am. Chem Soc.* **1992**, *114*, 2428. (b) Tarlov, M. J.; Newman, J. G. *Langmuir* **1992**, 8, 1398. (c) Huang, J.; Hemminger, J. C. *J. Am. Chem. Soc.* **1993**, *115*, 3342.

(11) (a) Huisgen, R.; Vossius, D.; Appl, M. *Chem. Ber.* **1958**, *91*, 1. (b) Huisgen, R.; Appl, M. *Chem. Ber.* **1958**, *91*, 12. (c) *Azides and Nitrenes*; Scriven, E. F. V., Ed.; Academic: San Diego, CA, 1984.

(12) Splitter, J. S.; Calvin, M. *Tetrahedron Lett.* **1968**, 1445.

(13) (a) Doering, W. von E.; Odum, R. A. *Tetrahedron* **1966**, *22*, 81. (b) Odum, R. A.; Wolf, G. *J. Chem. Soc., Chem. Commun.* **1973**, 360.

(14) Chapman, O. L.; Le Roux, J. P. *J. Am. Chem. Soc.* **1978**, *100*, 282.

(15) (a) DeGraff. B. A.; Gillespie, D. W.; Sundberg, R. J. *J. Am. Chem. Soc.* **1974**, *96*, 7491. (b) Shields, C. J.; Crisope, D. R.; Schuster, G. B.; Dixon, A. J.; Poliakoff, M.; Turner, J. J. *J. Am. Chem. Soc.* **1987**, *109*, 4723. (c) Li, Y. Z.; Kirby, J. P.; George, M. W.; Poliakoff, M.; Schuster, G. B. *J. Am. Chem. Soc.* **1988**, *110*, 8092. (d) Hayes, J. C.; Sheridan, R. S. *J. Am. Chem. Soc.* **1990**, *112*, 5879.

(16) (a) Leyva, E.; Platz, M. S. *Tetrahedron Lett.* **1985**, *26*, 2147. (b) Leyva, E.; Platz, M. S.; Persy, G.; Wirz, J. *J. Am. Chem. Soc.* **1986**, *108*, 3783. (c) Marcinek, A.; Levya, E.; Whitt, D.; Platz, M. S. *J. Am. Chem. Soc.* **1993**, *115*, 8609.

(17) (a) Soundararajan, N.; Platz, M. S. *J. Org. Chem.* **1990**, *55*, 2034. (b) Keana, J. F. W.; Cai, S. X. *J. Org. Chem.* **1990**, *55*, 3640.

(18) (a) Rupe, H.; Majewski, K. von *Ber. Dtsch. Chem. Ges.* **1900**, *33*, 3401. (b) Nielsen, P. E.; Buchardt, O. *Photochem. Photobiol.* **1982**, *35*, 317.

(19) (a) Ryan, M. A.; Spitler, M. T. *Langmuir* **1988**, *4*, 861. (b) Meijer, E. W.; Nijhuis, S.; Van Vroonvohen, F. C. B. M. *J. Am. Chem. Soc.* **1988**, *110*, 7209. (c) Cai, S. X.; Nabity, J. C.; Wybourne, M. N.; Keana, J. F. W. *Chem. Mater.* **1990**, *2*, 631. (d) McGarvey, C. E.; Holden, D. A. *Langmuir* **1990**, *6*, 1123. (e) Harmer, M. A. *Langmuir* **1991**, *7*, 2010. (f) Yan, M.; Cai, S. X.; Wybourne, M. N.; Keana, J. F. W. *J. Am. Chem. Soc.* **1993**, *115*, 814.

(20) (a) Lin, C.-H.; Wollman, E. W.; Wrighton, M. S. Unpublished results. (b) Wollman, E. W. Ph. D. Thesis, Massachusetts Institute of Technology, Cambridge, MA, 1992.

alization of surfaces with a monolayer of molecular reagents. Most importantly, irradiation of Au-I and Au-II SAMs in the presence of well-defined trapping reagents enables high lateral resolution patterning of Au surfaces with a broad range of molecular functionality. Patterned Au-I and Au-II SAMs are generated by irradiating the SAM through a mask and a thin film of a liquid reagent which produces the photoadduct only in irradiated portions of the substrate. By choosing the appropriate functionalized trapping reagent and photomask, arbitrary functional groups may be written onto the Au surface in any desired pattern. Our preliminary work detailing the use of scanning electron microscopy (SEM)[21] and secondary ion mass spectrometry (SIMS)[22] to image photochemical patterns in Au-I SAMs has been recently reported elsewhere.

Experimental Section

Materials. All starting materials and solvents (reagent grade or better) were purchased from commercial sources and used as received except for CH_3CN, THF, and hexanes, which were distilled from CaH_2, and diethylamine, which was distilled from KOH. Basic alumina (ICN Biomedicals) was allowed to equilibrate with the laboratory atmosphere to attain the same activity as alumina TLC plates.

Polycrystalline Au films were prepared by electron beam deposition of a 50 Å Ti adhesion layer followed by 1000 Å of Au on Si_3N_4 coated Si wafers. Au microstructures on Si_3N_4 consisted of 4 μm wide Au wires separated by 2 μm gaps and were fabricated using conventional lithographic techniques.[23] Each of the Au microwires could be individually contacted electrically via a macroscopic Au lead.

Synthesis. Procedures used to synthesize di-11-(4-azidobenzoate)-1-undecyl disulfide, **I**, 11-mercaptoundecylcyclopentadienylmanganese tricarbonyl, **II**, 2-ferrocenylethyl-2′,2′,2′-trifluoroethylamine, **III**, decyl-1,1-dihydropentadecafluorooctylamine, **IV**, 2-(2,6-dichlorophenyl)ethylpropylamine, **V**, methyl-4-azidobenzoate, **VI**, 2-(diethylamino)-5-(methoxycarbonyl)-3*H*-azepine, **VII**, *N*,*N*-diethyl-*N*′-(4-methoxycarbonyl)phenylhydrazine, **VIII**, methyl-4-aminobenzoate, **IX**, $PPh_2(CH_2)_{11}Fc$, **X**, and $PPh_2(CH_2)_2(CF_2)_5CF_3$, **XI**, and their spectroscopic properties are described in the Supplementary Materials for this article.

Mask Fabrication. The Cr-on-glass mask was fabricated at MIT and was originally designed for use in the fabrication of microelectrodes by standard lithographic techniques. The feature sizes on the mask range from 2–100 μm.

Instrumentation. All infrared spectroscopy was performed on a Nicolet 60SX FTIR spectrometer equipped with a liquid nitrogen cooled $Hg_xCd_{1-x}Te$ detector. Transmission spectra were obtained in CaF_2 or NaCl solution cells. RAIR spectra of the SAMs on Au were acquired with 70–82° angles of incidence using a polarizer to eliminate s-polarized light. Typically, at least 1000 scans at 4-cm^{-1} resolution were collected. Electrochemical measurements were performed in a 0.1 M $NaClO_4$ CH_3CN/H_2O (v:v, 1:1) electrolyte solution using a Pine Instruments RDE4 potentiostat and were recorded with a Kipp and Zonen BD90 XY chart recorder. All potentials are reported versus SCE. X-ray photoelectron spectroscopy (XPS) was performed using a Surface Science Instruments (Fisons) SSL-100 spectrometer with an Al $K\alpha_{1,2}$ source and a quartz monochromator. Peak positions are referenced to the Au $4f_{7/2}$ peak at 83.9 eV. The micrograph of the condensation figure (Figure 12) was obtained using a Mitutoyo optical microscope at 50X magnification. A Gaertner Scientific ellipsometer was used to measure the thickness of Au-I SAMs. Mass spectra were obtained using a Finnegan 8200 MAT system or an HP Model 5971A mass selective detector with a GC input. GC analyses were performed on either a Shimadzu Model GC-9A with a 15-m capillary methyl silicone column and an FID detector, or an HP Model 5890 capillary GC with a 12-m methylsilicone column interfaced to a Model 5971A mass selective detector. The initial column temperature was set to 150 °C and after 1 min was ramped to 250 °C at 20°/min. Injection port temperature was maintained at 200 °C or below to avoid thermal decomposition of the aryl azide. The typical injection volume was 1.5 μL.

Secondary Ion Mass Spectrometry.[22,24] All spectra and images were acquired using a Fisons (VG) IX70S magnetic sector SIMS instrument. The spectrometer was calibrated using a mixture of CsI, RbI, KI, NaI, and LiI salts dissolved in 3:1 $MeOH/H_2O$ and dispersed on a Au slide. The primary ion beam consisted of 16-keV Ga^+ ions generated from a liquid metal field emission source. Typical primary beam currents used in acquiring the mass spectra were 50 pA over a 10^{-3} cm^2 area, yielding primary beam current densities of 5×10^{-8} A cm^{-2}. Five scans, each 20 s in duration, were taken over five separate 10^{-3} cm^2 areas of the sample. The five scans were then averaged to give a composite spectrum. Total ion dose to each area was 3×10^{12} particles cm^{-2}. Mass resolution was 500.

Imaging SIMS was done using a 16-keV Ga^+ primary ion beam. Each map obtained is a 256 × 256 pixel image with a dwell time of 400 μs/pixel, so that each map took 26 s to acquire. The maps in Figure 4 are images of approximately 3.6×10^{-3} cm^2 areas and were obtained using a beam current density of 7×10^{-9} A cm^{-2}, corresponding to a total ion dose of 1×10^{12} particles cm^{-2}. The SIMS map in Figure 9 is an image of an approximately 1.3×10^{-4} cm^2 area and was obtained using a beam current density of 2×10^{-7} A cm^{-2}, corresponding to a total ion dose of 3×10^{13} particles cm^{-2}.

Scanning Electron Microscopy.[21] The SEM image was obtained using a Perkin-Elmer 660 scanning Auger spectrometer. The Auger instrument is capable of simply performing as a scanning electron microscope. The image was acquired using a 3-keV electron beam operating at 2 nA. Acquisition time for the image was 70 s.

Formation of Au-I SAMs. Au coated Si wafers previously described were fractured into 1.5 cm × 0.75 cm pieces and sonicated sequentially in ethanol, acetone, and water, followed by treatment in O_2 (8 min) and H_2 (3 min) rf plasmas (100 W). The cleaned Au substrates were then immediately immersed in a methylcyclohexane solution of **I** (~1 mM) upon removal from the plasma cleaner. The substrates were allowed to soak at least 2 h. The same procedure was followed for the derivatization of the Au microstructures previously described with disulfide **I**.

Solution Photochemistry of Methyl-4-azidobenzoate (VI). A quartz Schlenk tube with a stir bar was charged with 10 mg (0.056 mmol) of **VI**, 10 mg of hexadecane internal standard, and 50 mL of either neat diethylamine or THF with 5% diethylamine. The tube was sealed with a rubber septum, deoxygenated, placed before a 200W Oriel super high pressure Hg lamp with either a 260-nm long pass IR filter (water/ethanol/ethyl acetate 1:1:1) or a 320 nm long-pass filter with a water IR filter, and stirred. Aliquots for GC analysis were taken by syringe before and during the course of the photolysis. Concentrations of **VI**, 2-(diethylamino)-5-(methoxycarbonyl)-3*H*-azepine, **VII**, *N*,*N*-diethyl-*N*′-(4-methoxycarbonyl)phenylhydrazine, **VIII**, and methyl-4-aminobenzoate, **IX**, were calculated using extraction coefficients determined from standard solutions of **VI–IX**. For FTIR analysis, a 22.5 mM diethylamine solution of **VI** was prepared, deoxygenated, injected into an IR solution cell, and irradiated ($\lambda > 260$ nm) through the NaCl cell windows.

Photolysis of Au-I SAMs in the Presence of Amines. A 1.5 cm × 0.75 cm piece of derivatized Au was removed from the methylcyclohexane derivatizing solution, rinsed copiously with ethanol, acetone, hexane, and ethanol again, and then blown dry with N_2. Photolysis of Au-I in the presence of diethylamine was performed by immersing the Au-I substrate in deoxygenated diethylamine in a quartz tube under Ar and irradiating with a Bausch and Lomb SP 200 high-pressure mercury arc lamp for 2-min intervals ($\lambda > 280$ nm). Photolysis of Au-I in the presence of *N*-(2-ferrocenylethyl)-2′,2′,2′-trifluoroethylamine, **III**, was done by sandwiching a drop (~0.05 mL) of **III** between the Au-I substrate and a quartz plate and irradiating this assembly through the quartz. After irradiation, the Au substrates were rinsed with ethanol and then blown dry with N_2.

Photopatterning Au-I SAMs. Au microstructures on Si_3N_4 which were derivatized with **I** were photopatterned in a Karl Suss MJB contact aligner equipped with a 200 W Hg short-arc lamp (8 mW/cm^2 at 365 nm). The mask used in the aligner consisted of a Cr stripe about 1-cm wide on a quartz plate. A drop of the desired amine was placed on the substrate, and the Cr stripe on the mask was aligned with the substrate such that some of the microwires were completely covered. The mask was then brought into hard contact with the substrate, forcing the amine to spread evenly between the mask and the substrate. The assembly was irradiated ($\lambda > 285$ nm) through the mask for 10 min. The exposed substrates were

(21) Wollman, E. W.; Frisbie, C. D.; Wrighton, M. S. *Langmuir* **1993**, *9*, 1517.

(22) (a) Frisbie, C. D.; Wollman, E. W.; Martin, J. R.; Wrighton, M. S. *J. Vac. Sci. Technol.* **1993**, *A 11(4)*, 2368. (b) Frisbie, C. D.; Wollman, E. W.; Wrighton, M. S. Manuscript in preparation.

(23) (a) Smith, D. K.; Lane, G. A.; Wrighton, M. S. *J. Phys. Chem.* **1988**, *92*, 2616. (b) White, H. S.; Kittlesen, G. P.; Wrighton, M. S. *J. Am. Chem. Soc.* **1984**, *106*, 5375.

(24) (a) Frisbie, C. D.; Martin, J. R.; Duff, R. R.; Wrighton, M. S. *J. Am. Chem. Soc.* **1992**, *114*, 7142. (b) Frisbie, C. D.; Fritsch-Faules, I.; Wollman, E. W.; Wrighton, M. S. *Thin Solid Films* **1992**, *210/211*, 341.

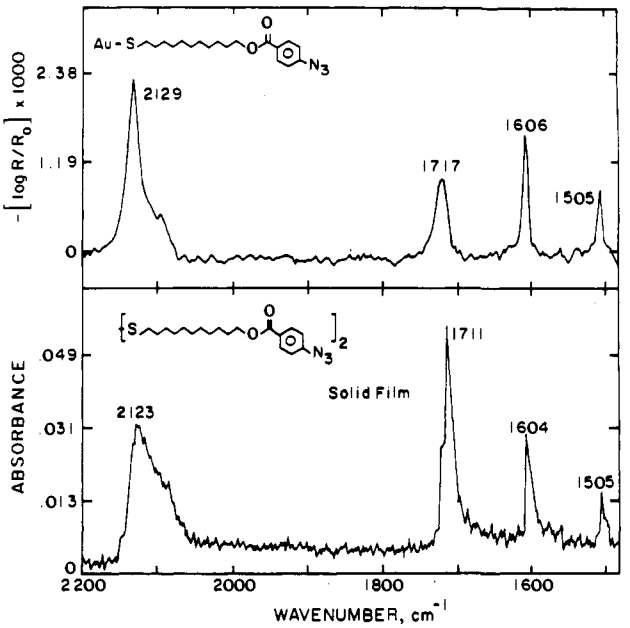

Figure 1. FT RAIR spectrum (8° angle of incidence, 8000 scans) of Au-I (upper) and IR transmission spectrum of an isotropic thin film of I (lower) showing the absorbances for azide (2125 cm^{-1}), ester (1717 cm^{-1}), and arene (1604, 1505 cm^{-1}).

cleaned by rinsing with acetone and ethanol and blown dry with N_2. This procedure was repeated in the presence of a second amine after moving the mask to expose the other microwires.

SAMs of I on flat polycrystalline gold films such as those used for the electrochemical and infrared experiments were patterned by irradiating the Au-I substrate with a Bausch and Lomb SP 200 high-pressure mercury arc lamp through the mask described above in the presence of a thin film of the desired amine. For the condensation figure shown in Figure 12, diethanolamine was used. The water was condensed onto the patterned film by placing the wafer on ice during photography.

Formation of Au-II SAMs. Au-coated Si wafers were cut into pieces approximately 0.5 cm × 2 cm and then cleaned by ultrasonication for 10 min in each of three solvents in order of increasing polarity: hexane, CH_2Cl_2, and EtOH. The ultrasonication was followed by plasma treatment in a Harrick PDC-23G plasma cleaner: 3 min in a flowing O_2 plasma, 0.3 Torr at medium power (40 W); 3 min in a flowing H_2 plasma, 0.5 Torr at low power (30 W). Functionalization of the clean Au surfaces was carried out by immersing the substrates into 1 mM solution of II in hexane for at least 2 h.

Photolysis of Au-II SAMs. A Au substrate was removed from solution containing II, rinsed with hexane, and allowed to dry in air. The Au surface then coated with a thin film of the appropriate liquid phosphine and placed in contact with either a glass microscope slide or the Cr side of the Cr-on-glass mask. Substrates coated with $PPh_2(CH_2)_2(CF_2)_5CF_3$ or $PPh_2(CH_2)_{11}Fc$ required occasional warming with a heat gun to prevent freezing of the phosphine.

The Au surface was irradiated through the slide or mask for 8–10 min with two Sylvania blacklight bulbs having maximum output ~355 nm. The substrate was afterwards separated from the mask and rinsed with hexane and THF. Some samples were immersed in 20% benzyl bromide in EtOH for 20 min to remove residual phosphine. Samples exposed to benzyl bromide were rinsed with clean EtOH prior to characterization.

Results and Discussion

Formation and Characterization of Au-I SAMs. Figure 1 shows the RAIR spectrum of a Au-I SAM, which contains peaks arising from azide (2125 cm^{-1}), ester (1720 cm^{-1}), and phenyl (1604, 1506 cm^{-1}) groups, and of a thin film of I, which has similar absorbances. An interesting feature of the spectrum of Au-I is that the oscillator strength (integrated absorbance) of the ester CO stretch (1720 cm^{-1}) is lower, relative to the other peaks, than in the spectrum of the isotropic thin film. This fact demonstrates the ordered nature of the Au-I SAM. For RAIRS of monolayer films on metallic surfaces, only the component of the electric field perpendicular to the metal surface has appreciable magnitude in the film.[25] Thus, only the component of the transition dipole (the CO bond in this case) normal to the surface will detectably attenuate the beam intensity. The relatively low oscillator strength of the CO stretch indicates that the bond is nearly parallel to the surface.[1a]

Using the integrated absorbances of the peaks at 2125, 1606, and 1506 cm^{-1}, the coverage of I was calculated[26] to be 2.6, 3.6 and 3.7 × 10^{-10} mol/cm^2, respectively. This is roughly half the coverage of $CH_3(CH_2)_{17}SH$ on Au,[1d] and about the same as the coverage for ferrocenyl terminated long chain alkanethiolates on Au.[1h] Ellipsometry showed the thickness of Au-I fims to be 23 ± 3 Å. Infrared spectroscopy and ellipsometry thus establish that disulfide reagent, I, Scheme 1, can be used to prepare photosensitive Au-I SAMs.

Scheme 2. Solution Photochemistry of Model Aryl Azide VI in the Presence of Secondary Amines (R = C_2H_5, C_4H_9)

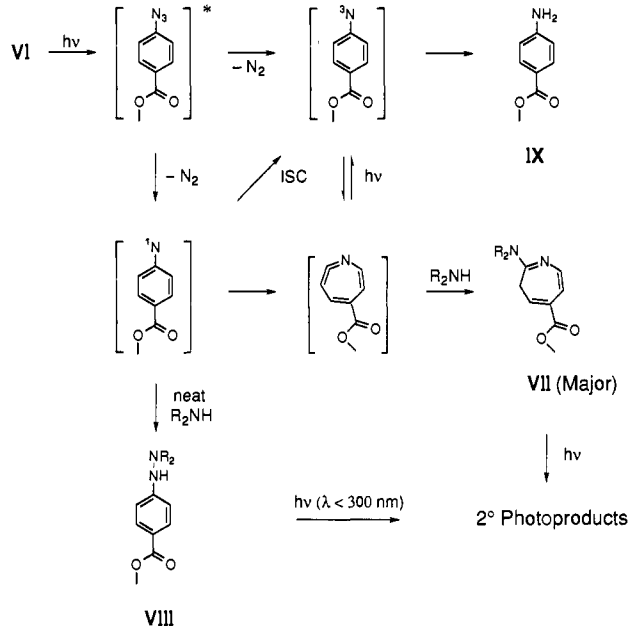

Solution Photochemistry of VI. The solution photochemistry of aryl azide derivatives has been extensively studied[11–18] and is characterized by the reactivity of singlet and triplet nitrene species formed from the photochemical loss of N_2 (Scheme 2). In the presence of amines, singlet phenyl nitrenes may be directly trapped to form phenyl hydrazines[17] or may undergo ring expansion to form 2-dehydroazepines,[14–17] which react rapidly with amines to ultimately form 2-amino-3*H*-azepines. 2-Dehydroazepines may also be produced via triplet phenyl nitrenes.[15d,16b] Other known products of triplet phenyl nitrenes include anilines.[16,17] The exact nature and distribution of the products of aryl azide photolysis, however, are sensitive to the arene ring substituents. No previous studies have reported in detail the products of photolysis of 4-azidobenzoates, such as the disulfide reagent, I, in the presence of amines. Because we were interested in establishing the surface-confined products upon irradiation of Au-I SAMs, we undertook solution photolysis studies of methyl 4-azidobenzoate, VI, to determine the possible photoproducts and their ratios.

(25) Greenler, R. G. *J. Chem. Phys.* **1966**, *44*, 310.

(26) The coverage was calculated using the following formula: $\Gamma = 1/2\alpha\omega^{-1}\cos\phi$, where ϕ is the angle of incidence of the beam, ω (cm^2·mol^{-1}) is the integrated isotropic extinction coefficient for the entire peak from a solution spectrum of a known concentration of I, and α is the value $-\log(R/R_0)$ integrated over the same frequencies as ω. A more rigorous theoretical treatment of the reflection of infrared radiation from a metal substrate coated with an absorbing thin organic film can be found in ref 25. In terms of calculating coverages, both treatments suffer from the lack of knowledge concerning the precise orientation of the dipole moments of the absorptions relative to the surface, cooperative effects on the absorptions, etc.

The product distribution of the photolysis of **VI** is dependent on the wavelengths of excitation and the concentration of amine. For example, irradiation ($\lambda > 260$ nm) of a 2 mM solution of **V** in neat diethylamine affords, at low conversions, azepine **VII**, hydrazine **VIII**, and aniline **IX** in a 7:2:2 ratio as primary photoproducts with a combined yield of 80%. If photolysis of **VI** ($\lambda > 260$ nm) is performed in a 5% THF solution of diethylamine instead, only **VII** and **IX** are observed initially in approximately a 3:1 ratio. Thus, increasing the concentration of the secondary amine allows the rate of the direct trapping of the singlet nitrene to form hydrazine to compete with the rate of ring expansion resulting in azepine. At later times in the photolysis, **VII** and **VIII**, which are light sensitive at these wavelengths, reach a maximum concentration and are then depleted, while **IX** continues to accumulate, the combined yield of **VII**, **VIII**, and **IX** at 90% conversion being only 60%.

Photolysis of **VII** to produce secondary photoproducts becomes even more important when longer wavelengths are used to irradiate solutions of **VI**. For example, irradiation of a 1 mM diethylamine solution of **VI** with longer wavelength light ($\lambda > 320$ nm) again affords **VII**, **VIII**, and **IX**, this time in a 4:2:1 ratio. At less than 30% conversion of the azide, their combined yield is 80%. However, at these wavelengths, photolysis of **VI** becomes extremely slow after 50% conversion, because **VII** has at least 20 times the extinction coefficient of **VI** at 325 nm. Accordingly, at later times using longer wavelength light, **VII** is nearly completely consumed to produce secondary photoproducts, while **VIII** and **IX** persist. Photolyses performed with dibutylamine in place of diethylamine and with more concentrated solutions of **VI** give similar results.

To summarize, we find that using shorter wavelength light, aryl azide **VI** is more selectively irradiated and efficiently converted to primary products azepine **VII**, hydrazine **VIII**, and aniline **IX**, while the secondary photolysis of **VII** and **VIII** is relatively slow. Irradiation of **VI** at longer wavelengths, while initially giving marginally higher yield of amine trapped photoproducts and preserving **VIII**, results in increased secondary photolysis of **VII**. The secondary photoproducts have not been identified in this study. Azepine photolysis has, however, been reported to yield bicyclic structures which maintain connectivity of the trapped amine to the original carbon skeleton of the aryl azide.[27] Thus, secondary photolysis should not result in loss of photoattached amine. This is consistent with XPS and cyclic voltammetry data for photolysis of Au-I in the presence of secondary amines, which indicate high coverage of trapped amine even after long periods of irradiation (*vide infra*).

Photolysis of **VI** in neat diethylamine was studied by FTIR for purpose of comparison to the RAIR spectrum of Au-I SAMs photolyzed through a thin film of diethylamine (*vide infra*). Irradiation ($\lambda > 260$ nm) of a 22.5 mM solution of **VI** in diethylamine results in the FTIR spectral changes shown in Figure 2 (upper), for which starting material has been removed by spectral subtraction, after approximately 20% conversion. The product peaks are assigned as a combination of **VII**, **VIII**, and **IX**, with the higher frequency portion of the CO absorption corresponding to **VII** and the lower frequency portion to **VIII** and **IX**, the arene peak at 1606 cm^{-1} corresponding to both **VIII** and **IX**, and the peak growing in at 1567 cm^{-1} corresponding only to **VII**, its absorbance indicating 70% yield. The N–H stretch region of the spectrum is obscured by solvent. At longer irradiation times peaks corresponding to neither **VII**, **VIII**, nor **IX** grow in at 1686, 1596, and 1525 cm^{-1}.

Photochemistry of Au-I SAMs Characterized by RAIRS, XPS, and Cyclic Voltammetry. The RAIR spectrum in Figure 2 (lower) shows that irradiation of Au-I SAMs ($\lambda > 260$ nm, ~2 min) in

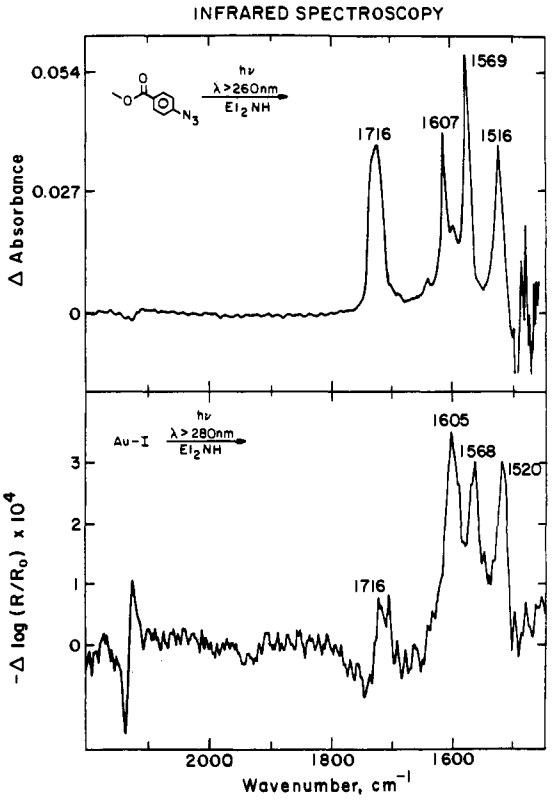

Figure 2. Difference FTIR spectrum showing product peaks for photolyses ($\lambda > 260$ nm) of a 22.5 mM diethylamine solution of **V** in a 0.02 cm NaCl IR cell after 1 min (upper) and a Au-I SAM ($\lambda > 280$ nm) in diethylamine after 2.3 min (lower).

the presence of diethylamine results in disappearance of the peak at 2125 cm^{-1} and appearance of new peaks at 1710, 1606, 1565, and 1520 cm^{-1}, which are assigned to the formation of surface confined analogues of **VII**, **VIII**, and **IX** by comparison with the solution spectrum in Figure 2 (upper). Further irradiation (8 min) of the Au-I surface results in disappearance of the peak at 1565 cm^{-1} and persistence of absorptions at 1710, 1606, and 1520 cm^{-1}. Interestingly, the ester carbonyl peak at 1710 cm^{-1} does not increase relative to the other peaks during photolysis, indicating that the ester CO bond remains oriented parallel to the substrate surface, and therefore that the aryl azide photochemistry does not disturb the monolayer ordering up to the ester carbonyl. Maintaining the integrity of the underlying long chain hydrocarbon support during photopatterning of photosensitive SAMs is an important prerequisite for defining surface properties by choice of trapping reagent. The RAIR spectrum in Figure 2 thus establishes that the primary surface-confined photoproducts are directly analogous to primary photoproducts **VII**, **VIII**, and **IX** obtained upon irradiation of **VI** in the presence of secondary amines.

The surface photochemistry of Au-I can also be followed semiquantitatively by X-ray photoelectron spectroscopy (XPS).[28,29] An XPS spectrum of Au-I contains a broad O(1s) peak near 532 eV, which can be fitted to two broad (FWHM = 2 eV) overlapping peaks at 531.3 and 532.5 eV, corresponding to the two ester oxygens. Two distinct N(1s) peaks due to the azide group are observed at 400.5 and 404.1 eV as shown in Figure 3 (upper).

(27) Odum, R. A.; Schmall, B. *J. Chem. Soc., Chem. Commun.* **1969**, 1299.

(28) *Practical Surface Analysis*; Briggs, D., Seah, M. P., Eds.; Wiley: New York, 1983.

(29) Aryl azide is sensitive to bombardment with energetic electrons.[30] Care must be taken to avoid decomposition of the aryl azide in Au-I during XPS fine structural analysis. An experiment during which the intensity of the N(1s) peak at 404.1 eV was monitored during continuous exposure to the X-ray source showed that decomposition occurred with a half life of 2 h when the largest spot size (1000 mm) was used. During the same time period no change in the O(1s) or Au(4f) signal was observed.

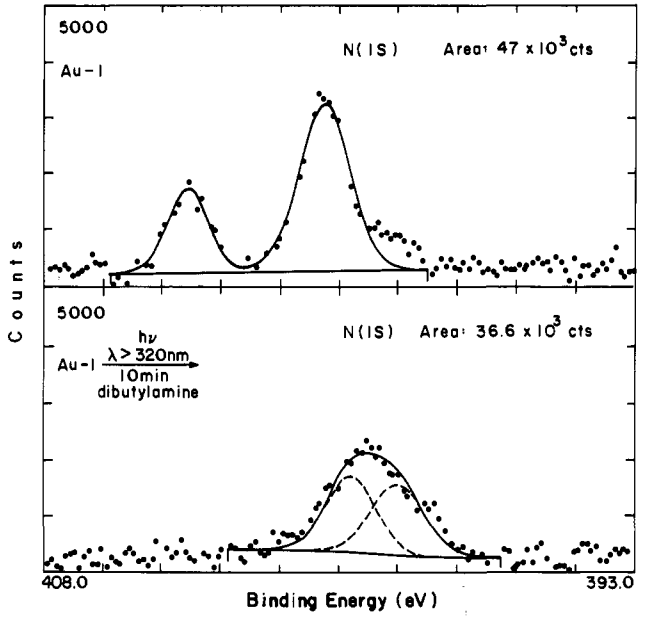

Figure 3. XPS analysis for the N(1s) region of samples of Au-I before (upper) and after (lower) irradiation through a thin film of dibutylamine.

The ratio of the areas of these two peaks is 2:1, the smaller peak corresponding to the relatively electron poor middle N atom of the azide group.[31] Analysis of Au-I SAMs irradiated in the absence of amine shows a single N(1s) peak, with 65% less N(1s) signal, consistent with the loss of N_2 from each surface-confined molecule in the irradiated SAM. XPS of Au-I after irradiation in the presence of **II** (Au-II) shows the unchanged O(1s) peak, consistent with conservation of ester linkage during photolysis, in addition to new peaks for F(1s) at 688.2 eV and Fe($2p_{3/2}$) at 707.2 eV. New peaks are also observed in the N(1s) region at 398.9 and 400.0 eV. The ratio, averaged over multiple experiments, of N(1s) counts between regions of Au-I and Au-II was about 3:1.62, indicating 62% yield of amine surface attachment, assuming validity of the stoichiometry in Scheme 1. The remaining 38% of product may be a surface-confined analog to aniline **IX**. By the same measurement, irradiation through dibutylamine gives a ratio of 3:1.88 or 88% yield of surface attachment. A spectrum of Au-I after irradiation through a film of dibutylamine is shown in Figure 3 (lower). XPS analysis of Au-I irradiated through films of other amines including diethanolamine and **V** give similar results.

The presence of ferrocene in **III** allows quantitative assessment of coverage of the Au-**III** photoproduct by cyclic voltammetry. Figure 4 shows three cyclic voltammograms obtained after irradiation of Au-I ($\lambda > 320$ nm) in the presence of **III** for 0, 0.5, and 14 min. The cyclic voltammogram corresponding to no irradiation shows that no dark reaction occurs between Au-I and -**III**. Ferrocene coverage increases to 3.3×10^{-10} mol/cm² after irradiation for 14 min, comparable to the $3.0–4.0 \times 10^{-10}$ mol/cm² obtained from treatment of Au with di(10-ferrocenecarbonyldecyl)disulfide.[11] The Au-III SAMs are durable enough that if the samples are stored in the dark at 25 °C, no change in the ferrocene coverage is detected after 90 days. The important point is that electrochemical data establish unambiguously that irradiation of Au-I SAMs in the presence of secondary amines results in attachment of approximately one monolayer of amine to the Au-I SAM.

Photochemistry of Au-II SAMs characterized by SIMS. We have previously reported the details of the photochemistry of

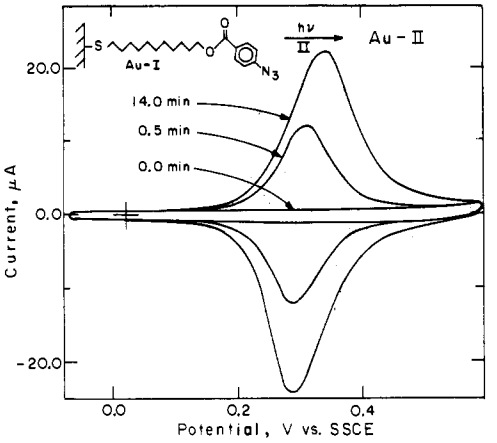

Figure 4. Cyclic voltammetry (Au macroelectrode, 0.1 M $NaClO_4$ in CH_3CN/H_2O, v/v 1:1, scan rate: 200 mV/s) of Au-I, photolyzed through a thin film of **III** sandwiched between the Au-I surface and a microscope slide, showing increasing coverage of surface-confined **III** with longer exposure. Coverages at 0.5 and 14 min are 1.6 and 3.3×10^{-10} mol/cm², respectively.

Au-II SAMs based on our studies by infrared spectroscopy and electrochemistry.[7] We are also interested in establishing whether secondary ion mass spectrometry (SIMS) can be used to detect the products of photochemical reactions in SAMs. In particular, surface mass spectral information obtained by SIMS should be useful in determining the structure of the surface-confined photoproducts in the same way conventional electron impact mass spectrometry is used to determine molecular structure of gas-phase molecules. Accordingly, we acquired SIMS survey spectra of Au-II SAMs irradiated in the presence of various phosphine trapping reagents.

Figure 5a shows a positive SIMS spectrum of Au-II after being exposed to $PPh_2(CH_2)_{11}Fc$ (**X**) in the dark. The major peaks are at m/z 55 and 252 and are assigned to Mn^+ and Au-Mn^+, respectively. Importantly, no peaks that can be assigned to ferrocene-containing fragments are observed, showing no thermal uptake of the phosphine. Figure 5b, however, shows a positive SIMS spectrum of Au-II after irradiation in the presence of **X**. The assignments of the important peaks are shown in the figure. The peaks at m/z 186, 199, 212, and 524 are particularly significant, since they correspond to fragments containing intact ferrocene.

Figure 6a shows a positive SIMS spectrum of Au-II after being exposed to $PPh_2(CH_2)_2(CF_2)_5CF_3$ (**XI**) in the dark. No peaks that can be assigned to F-containing species are observed. The minor differences between the Au-II surfaces in Figures 5a and 6a probably arise from differences in surface impurities and small differences in SIMS parameters. Figure 6b shows a positive SIMS spectrum of Au-II after irradiation in the presence of **XI**. The peaks at m/z 533 and 587 are critical, since they indicate the presence of the **XI** on the irradiated surface. The peak at m/z 587 also shows that coordination of **XI** to Mn occurs upon irradiation. Figures 5 and 6 demonstrate that there is no dark reaction of phosphines with Au-II SAMs but that attachment of phosphines to Au-II occurs upon irradiation. We believe that the fragments corresponding to intact **X** and **XI**, Figures 5b and 6b, represent detection of a monolayer of Mn-coordinated phosphine, and do not indicate the presence of adventitious free phosphine remaining on the Au-II substrate, for two reasons. First, if adventitious phosphine were left on the Au-II substrate, we would observe phosphine fragments from Au-II samples exposed to **X** and **XI** in the dark, Figures 5a and 6a, respectively. Second, cyclic voltammetry studies in our previous work[7b] have established that no more than one monolayer of redox-active ferrocene is found on Au-II substrates irradiated in the presence of **X**, eliminating the possibility that multilayers of phosphines are left

(30) (a) Marletta, G.; Pignataro, S.; Toth, A.; Bertoti, I.; Szekely, T.; Keszler, B. *Macromolecules* **1991**, *24*, 99. (b) Labinis P. E.; Graham, R. L.; Biebuyck, H. A.; Whitesides, G. M. *Science* **1991**, *254*, 981.

(31) The middle nitrogen atom bears a positive charge in both of the reasonable Lewis structures that can be drawn for phenyl azide.

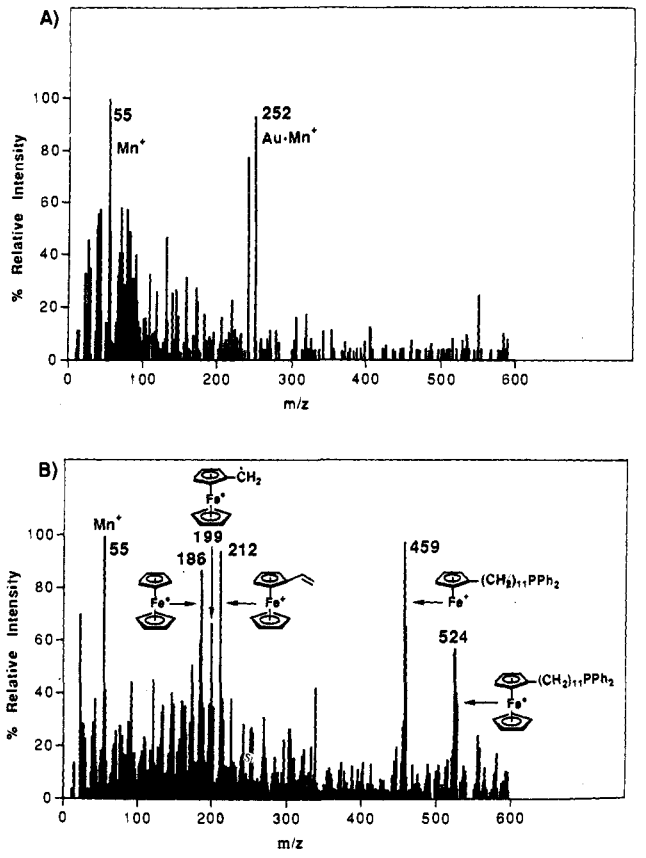

Figure 5. (A) Positive SIMS spectrum of Au-II treated with $PPh_2(CH_2)_{11}$-Fc in the dark. (B) Positive SIMS spectrum of Au-II irradiated in the presence of $PPh_2(CH_2)_{11}Fc$.

on the surface after irradiation. The intact phosphine fragments shown in Figures 5b and 6b must therefore arise from cleavage of the Mn–P bond of the surface-confined photoproducts, with subsequent ionization of the phosphine, either by $1e^-$ oxidation in the case of **X** or by H^+ abstraction in the case of **XI**, to yield positively charged molecular fragments $PPh_2(CH_2)_{11}Fc^+$, m/z 524 in Figure 5b, and $HP^+Ph_2(CH_2)_2(CF_2)_5CF_3$, m/z 533 in Figure 6b, respectively.

Observation of a molecular fragment containing a phosphine ligand plus all or a portion of **II** minus CO would offer direct evidence of a 1:1 photoadduct and serve to confirm the chemistry as depicted in Scheme 1, which has been established previously.[7] Figures 7a,b show positive SIMS spectra of Au-II after irradiation with UV light in the presence of PPh_2Et or $PPh_2(n\text{-}Pr)$, respectively. The assignments of the important peaks are noted in the figure. The peaks at m/z 269, 347, 466 in Figure 7a and m/z 283, 361, 480 in Figure 7b are noteworthy, since they correspond to fragments in which phosphine is coordinated to the Mn center. Importantly, we find the expected shift of 14 mass units in these key mass spectral features upon change of the photoattached phosphine from PPh_2Et to $PPh_2(n\text{-}Pr)$, Figure 7 (part a vs part b), and the correlation between these two sets of peaks confirms their respective assignments. The important point is that a significant molecular fragment of **II**, $CH_2(\eta^5\text{-}C_5H_4)Mn^+$, plus a phosphine ligand, at m/z 347 and 361, is observed in Figure 7, parts a and b, respectively. Peaks at m/z 269 and 283, corresponding to Mn^+–PPh_2Et and Mn^+–$PPh_2(n\text{-}Pr)$, also provide further evidence for the attachment of phosphine to the dicarbonyl Mn center on the irradiated surface. An electron-impact mass spectrum of $(\eta^5\text{-}C_5H_5)Mn(CO)_2PPh_3$ shows a peak at m/z 382, corresponding to $(\eta^5\text{-}C_5H_5)MnPPh_3^+$, analogous to peaks at m/z 347 and 361 in Figure 7a,b, respectively, and supports the conclusion that the SIMS spectra in Figure 7 confirm the presence of a 1:1 photoadduct on the Au surface.

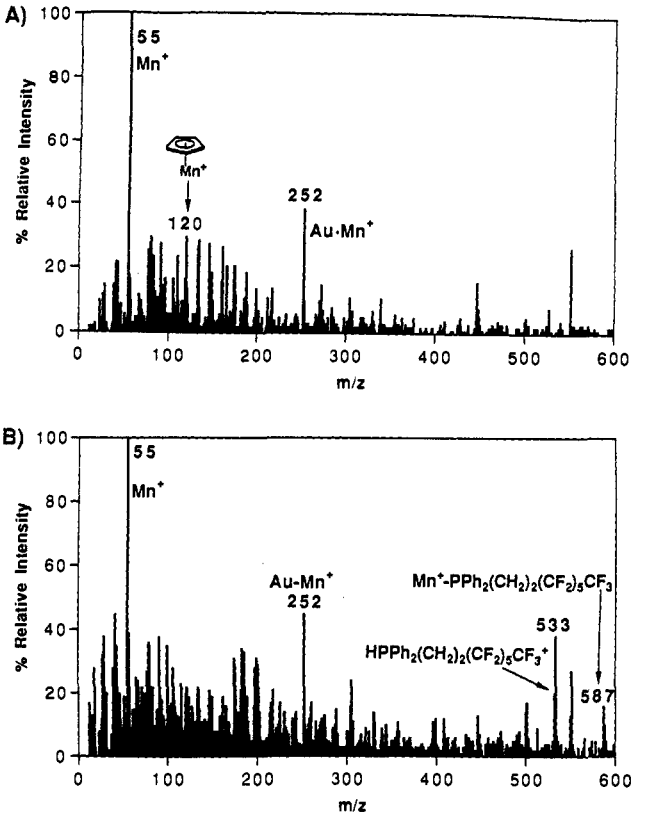

Figure 6. (A) Positive SIMS spectrum of Au-II treated with $PPh_2(CH_2)_2(CF_2)_5CF_3$ in the dark. (B) Positive SIMS spectrum of Au-II irradiated in the presence of $PPh_2(CH_2)_2(CF_2)_5CF_3$.

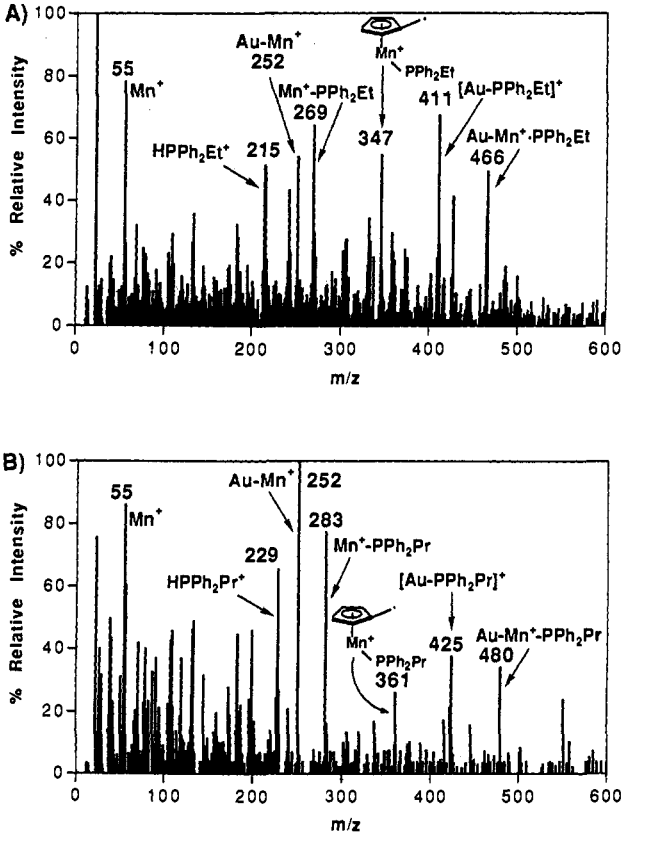

Figure 7. Positive SIMS spectra of Au-II irradiated in the presence of (A) PPh_2Et or (B) $PPh_2(n\text{-}Pr)$.

The peaks in Figures 5–7 that have been assigned to Au-containing species deserve some explanation. In general, SIMS

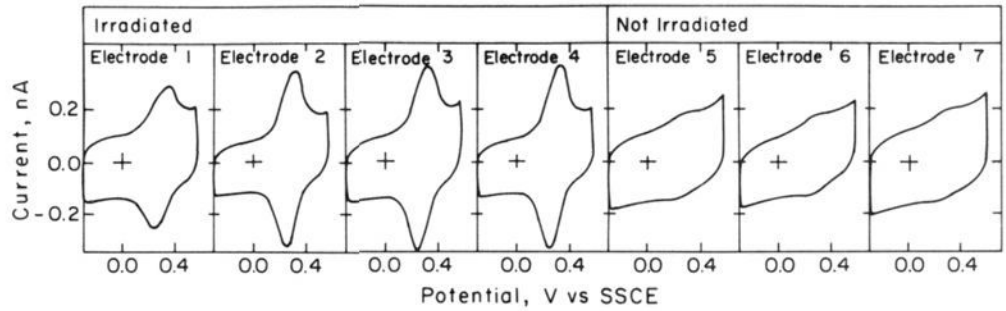

Figure 8. Cyclic voltammetry (0.1 M $NaClO_4$ in H_2O, scan rate: 500 mV/s) of Au-**I** on a Au microelectrode array, photolyzed through a film of **III** and a Cr-on-glass mask, showing that coverage of ferrocene on the microelectrodes reproduces the pattern of irradiation. ($\Gamma_{irradiated} = 1.0 \times 10^{-10}$ mol/cm^2; $\Gamma_{not\ irradiated} < 0.05 \times 10^{-10}$ mol/cm^2.)

spectra are complicated by the presence of ions which result from gas-phase reactions between fragment ions and substrate atoms, in this case Au. These reactions occur in the space immediately above the analysis area (termed the selvedge) before mass selection and detection in the spectrometer and can thus result in detection of ions which have no relation to the molecular structure of the original sample. The peak at m/z 252 in Figures 5a and 6a provides an illustrative example. Although there is no direct Au–Mn bond in Au-**II** SAMs, SIMS spectra of Au-**II** SAMs exposed to phosphine in the dark show a peak at m/z 252 which we assign to Au–Mn^+. Likewise, peaks assigned to Au–Mn^+, [Au–PPh_2R]$^+$, and Au–Mn^+–PPh_2R are observed in Figure 7a,b. The presence of these artifacts, however, does not detract from the utility of SIMS in providing detailed molecular structural information about photolyzed SAMs. Independent of any other technique, SIMS can establish the photochemistry of Au-**II** SAMs depicted in Scheme 1.

Photopatterning of Au-I and Au-II SAMs. Our primary motivation for developing photosensitive SAMs such as Au-**I** and Au-**II** is our interest in patterning surfaces with molecular functionality at high lateral resolution. The data shown in Figure 8 demonstrate our ability to use Au-**I** SAMs to selectively modify Au microstructures on a Si_3N_4 substrate. The microstructures consist of an array of seven 4.0 μm × 200 μm Au wires separated by ~2.0 μm. Immersion of the microfabricated substrate in a methylcyclohexane solution of **I** results in attachment of **I** selectively to the Au and not the Si_3N_4 substrate. Subsequent irradiation ($\lambda > 280$ nm, 15 min) of four of the microwires, through a Cr-on-glass mask and a thin film of pure **III**, results in the selective formation of Au-**III** on the four irradiated wires, as is shown by the electrochemical response of each of the wires (Figure 8). Ferrocene coverage on the three wires not irradiated is less than 1/20th that of the irradiated wires. The small ferrocene signals observed on wires 5–7 likely result from photoattachment arising from scattered light. In this example, we have used electrochemistry to demonstrate selective photopatterning.

Recently, we have also begun investigating the use of chemically sensitive microscopies such as scanning Auger microscopy[32] and imaging SIMS[22,24] for imaging the lateral distribution of surface-confined molecules. Imaging SIMS has been particularly fruitful in this regard. For example, Figure 9 shows SIMS maps for $^{35}Cl^-$ and $^{19}F^-$ ions which highlight the lateral distribution of amines **IV** and **V**, which were sequentially photopatterned onto a microwire array similar to the one described above. Inspection of the data shows that the SIMS maps confirm the conclusion made from the electrochemical data in Figure 8, namely, that masked irradiation of the Au microstructures results in selective attachment of amines to the irradiated wires. Furthermore,

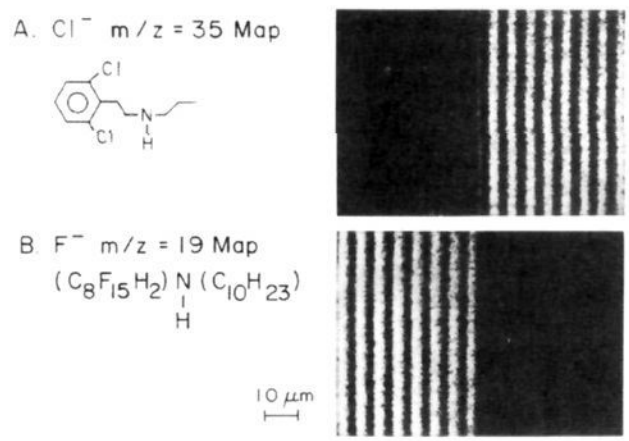

Figure 9. SIMS Cl^- and F^- maps (using a 12 pA, 25 keV Ga^+ primary ion beam) of a Au microelectrode array on a Si_3N_4 substrate treated to form Au-**I**, irradiated through a mask covering the microwires on the right in the presence of **IV**, and then irradiated in the presence of **V** with the mask covering the wires on the left. The maps show that adjacent portions of one wire have been treated with **IV** and **V**.

because the SIMS maps in Figure 9 show that F and Cl are present only on wires irradiated in the presence of **IV** and **V**, respectively, it is clear that no dark reaction occurs to attach amines to films of **I**. It is interesting to note in Figure 9 that in the initial irradiation the mask did not only cover the seven microwires on the left, as intended, but also a portion of an eighth microwire in the center. This misalignment resulted in photoattachment of **IV** and **V** to adjacent portions of the center microwire. The lateral resolution of imaging SIMS is adequate to detect this, as can be seen by the very thin strip in the center of the Cl^- map and the narrow strip in the F^- map. The conclusion from Figures 8 and 9 is that Au-**I** photochemistry can be used to selectively pattern adjacent Au microstructures at high lateral resolution. In principle, each of the microwires in the array could be functionalized with a different amine by employing a mask which exposes only a 4-μm wide strip and irradiating a different microwire each time a film of new amine is applied. Imaging SIMS could then be used to detect the different chemical functionalities of each wire.

Imaging SIMS may also be used to demonstrate photopatterning of Au-**II** SAMs on flat Au substrates. Figure 10a shows a SIMS map of the lateral distribution of vinyl ferrocenium (m/z 212) for a flat Au-**II** substrate (no prefabricated microstructures) after irradiation through a Cr-on-glass mask in the presence of $PPh_2(CH_2)_{11}Fc$. Only the region within the cross feature was irradiated, and the light area corresponds to the region where high surface coverage of ferrocene centers is detected by SIMS. Analysis of pixel intensities indicates the presence of about 20 times more of the ferrocene-containing fragment in the irradiated areas of the surface than in the nonirradiated regions. Figure 10b is a SIMS map for F^- (m/z 19) of Au-**II** irradiated through

(32) (a) Hickman, J. J.; Ofer, D.; Zou, C.; Wrighton, M. S.; Laibinis, P. E.; Whitesides, G. M. *J. Am. Chem. Soc.* **1991**, *113*, 1128. (b) Laibinis, P. E.; Hickman, J. J.; Wrighton, M. S.; Whitesides, G. M. *Science* **1989**, *245*, 845. (c) Hickman, J. J.; Zou, C.; Ofer, D.; Harvey, P. D.; Wrighton, M. S.; Laibinis, P. E.; Bain, C. D.; Whitesides, G. M. *J. Am. Chem. Soc.* **1989**, *111*, 7271.

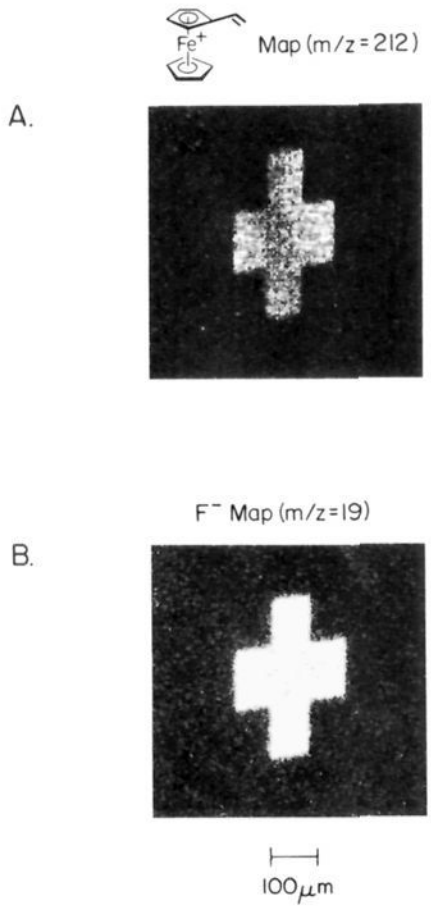

Figure 10. SIMS maps for (A) vinyl ferrocenium (m/z 212) or (B) F^- (m/z 19) of Au-**II** substrates irradiated through a mask in the presence of (A) $PPh_2(CH_2)_{11}Fc$ or (B) $PPh_2(CH_2)_2(CF_2)_5CF_3$. The light areas correspond to regions where counts were detected.

the Cr-on-glass mask in the presence of **XI**. Again, only the regions inside the cross feature were irradiated, and the light areas corresponds to the regions where F^- is detected by SIMS. About 100 times more F^- was detected in the irradiated areas of the surface than in the nonirradiated regions. Both maps in Figure 10 demonstrate that molecular functionality can be attached to the irradiated portions of the Au-**II** SAM with very good selectivity and modest resolution ($\sim$100 μm).

Figure 11a shows a SIMS map at higher magnification of the distribution of F^- from Au-**II** after irradiation through a mask in the presence of **XI**. The substrate was irradiated within the banded regions, and the light areas correspond to regions where F^- was detected. The fine lines in the figure are 2-μm wide and are spaced 2-μm apart, replicating the pattern of the Cr-on-glass mask. Thus, our monolayer photochemistry can be used to pattern surfaces with at least 1-μm resolution. In principle, patterns with lateral dimensions as small as several hundred nanometers could be patterned onto Au-**II** surfaces by UV irradiation through an appropriate mask. An important question, however, is whether such small patterns in a monolayer of material could be imaged by SIMS. In principle, SIMS can be used to resolve 100–200-nm features.[33] However, the practical limit for imaging SIMS of monolayers is probably $\sim$1 μm, owing to signal-to-noise constraints and ion beam-induced damage. The map in Figure

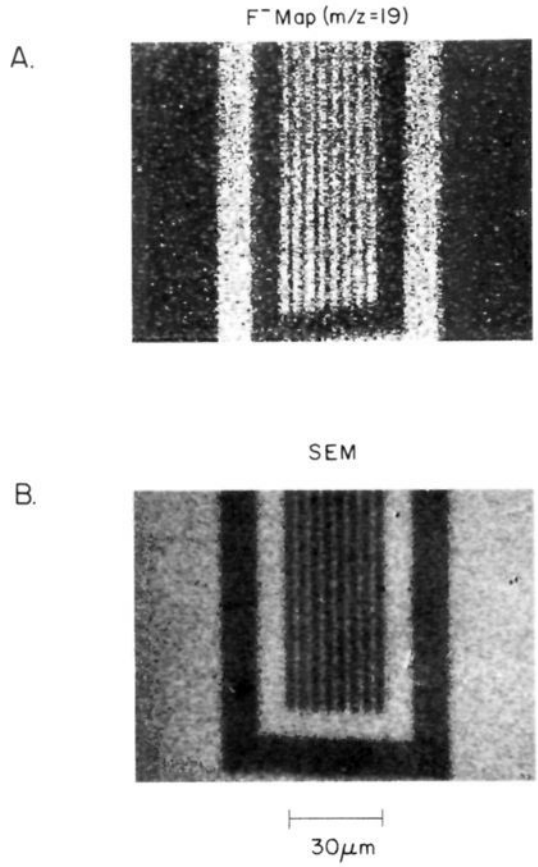

Figure 11. (A) SIMS map for F^- (m/z 19) of a Au-**II** substrate irradiated through a mask in the presence of $PPh_2(CH_2)_2(CF_2)_5CF_3$. The light areas correspond to regions where counts were detected. (B) SEM of the substrate shown in part (A).

11a showing 2-μm features therefore represents very high lateral resolution in terms of SIMS analysis.

We, and others, have also shown previously that scanning electron microscopy (SEM) can be used to image patterned monolayers. Figure 11b is a SEM image of a Au-**II** SAM irradiated in the presence of **XI**, analogous to the sample mapped by SIMS in Figure 11a. The SEM image confirms that clean photochemical patterning of Au-**II** has been achieved with a lateral resolution of 2 μm. An advantage of SEM over SIMS in imaging monolayers is that SEM is presently capable of imaging at much higher lateral resolutions. Features smaller than 50 Å (0.005 μm) can be resolved by SEM,[34] although we are not certain of the ability to obtain this resolution when imaging monolayers, owing to the associated electron beam damage. The SEM image in Figure 11b therefore confirms prior reports on SEM imaging of monolayers[21,35] but probably does not represent the best possible lateral resolution. Of course, it should be noted that while SEM allows for imaging at significantly higher lateral resolutions than SIMS, it offers no information about the chemical composition of surface species. In conclusion, Figures 10 and 11 show that Au-**II** substrates can be photochemically patterned with unique functional groups present in the incoming phosphine and with high lateral resolution. Our results also clearly demonstrate the utility of SIMS for characterizing Au-**II** SAMs photopatterned with functionalized phosphines.

Flat Au surfaces derivatized with **I** may also be patterned by irradiation through a mask in the presence of amines. The resulting patterns can be imaged by SEM[21] and SIMS.[22,24] A

(33) (a) Benninghoven, F. G.; Rudenauer, F. G.; Werner, H. W. In *Secondary Ion Mass Spectrometry: Basic Concepts, Instrumental Aspects, Applications, and Trends*; Elving, P. J., Wineforder, J. D., Eds.; Wiley: New York, 1985. (b) Vickerman, J. C.; Brown, A.; Reed, N. M. *Secondary Ion Mass Spectrometry: Principles and Applications*; Clarendon: Oxford, UK, 1989.

(34) Seiler, H. *J. Appl. Phys.* **1983**, *54*, R1-R18.

(35) Lopez, G. P.; Biebuyck, H. A.; Whitesides, G. M. *Langmuir* **1993**, *9*, 1513.

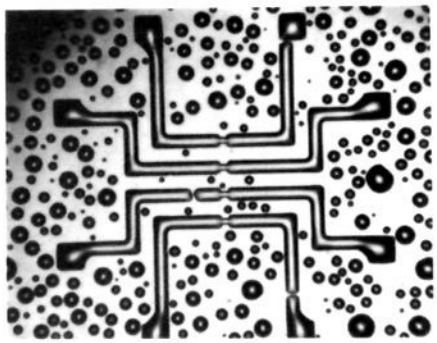

Figure 12. Optical micrograph of atmospheric water condensing onto a Au-**I** surface after photolysis through a mask and a film of diethanolamine. The water preferentially wets the irradiated regions which have hydrophilic OH termini and makes visible photopatterning of one monolayer.

simpler and nondestructive method for imaging patterned monolayers based on the relative hydrophilicities of different SAMs was recently described by Whitesides and co-workers.[2b] They showed that the condensation of water vapor onto patterned SAMs cooled in humid air produces images, called condensation figures or breath patterns, which display remarkably high contrast. The contrast is based upon the fact that water droplets nucleate and grow preferentially on hydrophilic surfaces. As established by other methods above, photopatterning SAMs of Au-**I** in the presence of an amine essentially changes the 4-azidobenzoate termini of the SAM to those of the amine. Since terminal functional groups of SAMs determine their wetting properties,[2] condensation figures should be ideal for the imaging of photopatterned Au-**I** SAMs. Figure 12 shows the condensation figure for a Au-**I** surface irradiated through a mask in the presence of diethanolamine. The photoattached diethanolamine renders the irradiated surface regions more hydrophilic than the native Au-**I** regions. When the photopatterned substrate is cooled, water vapor condenses on the patterned surface, highlighting the diethanolamine-containing regions of the surface. The condensation figure clearly resolves 50-μm features at the center of the micrograph and provides an elegant illustration of the use of Au-**I** photochemistry to pattern surfaces with molecular reagents at high lateral resolution.

Conclusions

Irradiation of Au surfaces modified with Au-**I** SAMs through thin films of secondary amines results in photoattachment of amines to the surface only where irradiated. By RAIRS, XPS, and cyclic voltammetry, we have established that the surface photochemistry proceeds via the formation of azepines, hydrazines, and anilines resulting in approximately monolayer coverages of surface-confined amine. Contact lithography can be employed to pattern functionalized amines on the Au-**I** surface with high lateral resolution, as determined by microelectrochemistry, SIMS, and condensation figures.

We also conclude from our work that the chemical properties of $(\eta^5\text{-}C_5H_4R)Mn(CO)_3$ can be exploited for the purpose of photochemically patterning surfaces with widely varying functional groups at high lateral resolution. Au-**II** surfaces are readily patterned because the tricarbonyl is thermally inert but undergoes efficient photinduced CO substitution. Our results suggest that Au-**II** substrates can, in principle, be patterned using any stable functional group bound to a phosphine or perhaps to other suitable $2e^-$ donors. Selective irradiation of substrates functionalized with **I** and **II** is therefore a general means of creating chemically patterned surfaces.

Acknowledgment. We wish to acknowledge the Office of Naval Research and National Science Foundation for partial support of this work. We appreciate the help of Ingrid Fritsch-Faules and Tim Gardner for providing the microelectrochemical devices used in this work, and we thank Timothy McClure and Richard Perilli for assistance at the MIT Microelectronics Laboratory. We would also like to thank Hans Biebuyck (Department of Chemistry, Harvard University) for introducing us to the use of condensation figures for imaging photopatterned monolayers.

Supplementary Material Available: Synthesis and spectroscopic characterization of compounds **I**–**XI** (6 pages). This material is contained in many libraries on microfiche, immediately follows this article in the microfilm version of the journal, and can be ordered from the ACS; see any current masthead page for ordering information.